Devices for Gradient Static Magnetic Field Exposure

Stefan Engström,[1]* Marko S. Markov,[2] Michael J. McLean,[1] Robert A. Jones,[3] and Robert R. Holcomb[1]

[1]Department of Neurology, Vanderbilt University, Nashville, Tennessee
[2]Research International, Buffalo, New York
[3]Inland Technical Services, San Bernardino, California

We describe devices designed for magnetic field exposures in which field amplitude and gradients are controlled simultaneously. Dosimetry based on field continuation of high resolution magnetic field scans and numerical models is compared with validation measurements. The dosimetry variables we consider are based on the assumption that the biological or chemical system under study has field transducers that are spatially isotropic, so that absolute field amplitude and two gradient components fully describe local exposure. Bioelectromagnetics 26:336–340, 2005. © 2005 Wiley-Liss, Inc.

Key words: dosimetry; myosin phosphorylation; exposure system; DC magnetic field

INTRODUCTION

The design of these exposure devices has its origin in observations that a square array of four magnets with alternating polarity (MagnaBloc, US patent no. 5 312 321) has the ability to reversibly block action potentials in cultured dorsal root ganglia neurons [Cavopol et al., 1995; McLean et al., 1995] and that this effect is dependent on gradient properties of the field. Neither the effective metric nor the mechanism of action is known, but it was observed that the most biologically effective region lies near a point located in the symmetry plane between adjacent pairs of magnets. Everywhere in this plane, the field vector is perpendicular (normal) to the symmetry plane and it follows that the gradient of the field magnitude lies entirely in this plane. This, as well as the need to simplify the characterization of the many parameters needed to fully describe the field and gradients, guided how we parameterize the field (*cf.* ''Field Parameterization'').

In experiments on the rate of myosin phosphorylation [Engström et al., 2002] using this same square array of magnets, it was again seen that gradients played a role in the observed effects on this biochemical system. Furthermore, the experiments indicated that the physical transduction mechanism could not be explained with a single factor (field or gradient amplitude) model. A drawback of using the relatively small magnet array for field exposures was that the distribution of fields and gradients in the experimental volume was quite wide in the myosin phosphorylation experiment. The standard deviation of these parameters was comparable to their means in this experiment.

The very small exposure volume for the single neuron experiments [McLean et al., 1995] did not suffer from wide field distributions, but fields and gradients varied significantly on millimeter scales, so other uncertainties were introduced due to positioning of the cells in the field. Additionally, the fixed arrangement of permanent magnets provides a limited range of possible field and gradient parameters for exploration. This prompted the development of novel devices with larger permanent magnets that would have greater flexibility in their geometrical configuration so as to allow a wider range of exposure conditions. These new devices permit near-independent control of field amplitude and two gradient components with relatively small variability on mm scales. The larger physical dimensions of the magnets and their greater separation enable relatively

*Correspondence to: Stefan Engström, Department of Neurology, 2100 Pierce Avenue, Nashville, TN 37212.
E-mail: stefan.engstrom@vanderbilt.edu

tighter definition of these parameters as long as we keep the exposure volumes small compared to the dimensions and separation of the magnets.

THEORETICAL BACKGROUND

We are interested in creating gradient magnetic fields to expose biological and biochemical samples and to evaluate the effects of spatially inhomogeneous fields on these systems. Restricting ourselves to a volume in which the current density vanishes, the basic equations of magnetostatics are [Jackson, 1999]: $\vec{\nabla} \cdot \vec{B} = 0$, and $\vec{\nabla} \times \vec{H} = 0$, where $\vec{B}$ is the magnetic flux density, $\vec{H}$ the magnetic field, and arrows over variables and operators indicate vectors. The second relation implies that we can define a magnetic scalar potential Φ, such that: $\vec{H} = -\vec{\nabla}\Phi$. If the medium we consider is linear and isotropic, which will be a good approximation for most non-ferromagnetic materials, the constitutive relation is simply $\vec{B} = \mu\vec{H}$, and consequently $\vec{B} = -\mu\vec{\nabla}\Phi$. There are some useful relations between gradient components that follow:

$$\frac{\partial B_x}{\partial y} = -\mu\frac{\partial^2 \Phi}{\partial x \partial y} = -\mu\frac{\partial^2 \Phi}{\partial y \partial x} = \frac{\partial B_y}{\partial x} \qquad (1)$$

with similar relations for the pairs (x,z) and (y,z).

The existence of the magnetic scalar potential also permits continuation of the field using methods described previously [Engström, 2001]. Briefly, an extensive planar scan or calculation of the normal (perpendicular to the scan plane) component of the magnetic field allows the calculation of all properties of the magnetic field in a volume above the scanned plane. For example, if an extensive scan of B_z in the plane $z_0 = 0$ is available one can calculate all field components above that plane using Equation 2:

$$B_p(x, y, z)$$
$$= \frac{1}{2\pi}\iint \frac{(p - p')B_z(x', y', z_0)}{((x - x')^2 + (y - y')^2 + (z - z')^2)^{3/2}}\,dx'dy' \qquad (2)$$

where p is one of $\{x,y,z\}$.

FIELD PARAMETERIZATION

A complete description of the field conditions requires three vector components for the magnetic flux density $(\vec{B})$. The scalar equation $\vec{\nabla} \cdot \vec{B} = 0$ provides one constraint and three more are supplied by the vector relation $\vec{\nabla} \times \vec{H} = 0$. Thus, the nine components of the gradient tensor are reduced to five independent components after these constraints are taken into

account. Three field and five gradient parameters still present an unwieldy system to work with, and for this reason we have chosen to introduce an assumption of isotropy for the exposure target system. If we do assume that the ensemble of physical field transducers of the biological/chemical system under study is spatially isotropic, it follows that it is sufficient to consider only the scalar field amplitude $(B_a = \sqrt{\vec{B} \cdot \vec{B}})$ instead of the full field vector since all relative orientations of transducers and the field vector $(\vec{B})$ will be present in the ensemble, regardless of the field orientation. Similarly, we can consider the gradient of the field amplitude instead of the five independent gradient $(\vec{\nabla}B_a)$ components.

Consistent with the assumption of isotropy, it is possible to further reduce the number of parameters required for a complete description by considering the components of the field amplitude gradient $(\vec{\nabla}B_a)$ that are parallel and perpendicular to the local field vector, the only relevant orientation if other forces are not contributing significantly to the transduction or the organization of the system. This assumption is likely to be very good for systems in liquid solution, but could be questioned if there is structural detail, such as cells growing on the bottom of a culture dish, or if there is another relevant force present. It should be noted that the assumption of isotropy requires that the applied field does not significantly align the field detectors.

In the cases where the isotropy assumption is acceptable, we get a complete local description of the field and gradient situation with only three parameters: the amplitude of the magnetic field $(B_a = |\vec{B}|)$, the gradient components parallel $(G_p = (\vec{B} \cdot \vec{\nabla}B_a)/B_a)$ and perpendicular $(G_q = \sqrt{|\vec{\nabla}B_a|^2 - G_p^2})$ to the local field vector. The field (flux density) amplitude is measured in tesla (T), gradients in tesla/meter (T/m).

DEVICE DESIGN

As mentioned in the "Introduction," in previous experiments [McLean et al., 1995] it was noted that the largest biological effect was seen above the symmetry line where magnets in the MagnaBloc square array were touching. Expressing the field in the three parameters (B_a, G_p, G_q) we observed that the field in that area could be characterized as having a gradient component predominantly perpendicular to the local field vector $(G_q \gg G_q)$. Wanting to explore this type of field condition, we capitalized on the fact that the magnetic field in a symmetry plane ("A" in Fig. 1) between two magnets with their magnetization oriented as shown in that figure, has this property. In this plane the field vector is everywhere normal to the plane "A," and the
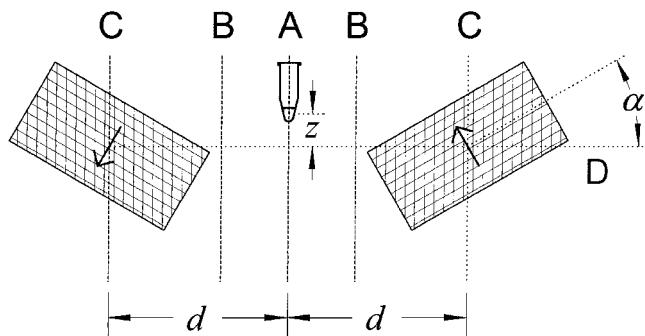
Fig. 1. Schematic representation of the gradient field exposure device. Two cylindrical NdFeB magnets (hatched, shown in cross-section) are mounted symmetrically about the plane "A" such that their center separation (2d), and their rotation angle (α) can be precisely controlled. The distance (z) from the center of the exposure volume (illustrated here with an Eppendorf tube) to the magnet centerline can also be manipulated to achieve different combinations of field and gradient conditions. The magnetization of the magnets is indicated with arrows in their respective center. With this configuration, the symmetry plane "A" has gradients that are everywhere perpendicular to the local field vector ($G_p = 0$). "B" marks the plane in which the normal component of the magnetic field was scanned for the field continuation calculations for device no. 1. The intersection of planes "C" and "D" defines the axes about which the magnets can rotate.
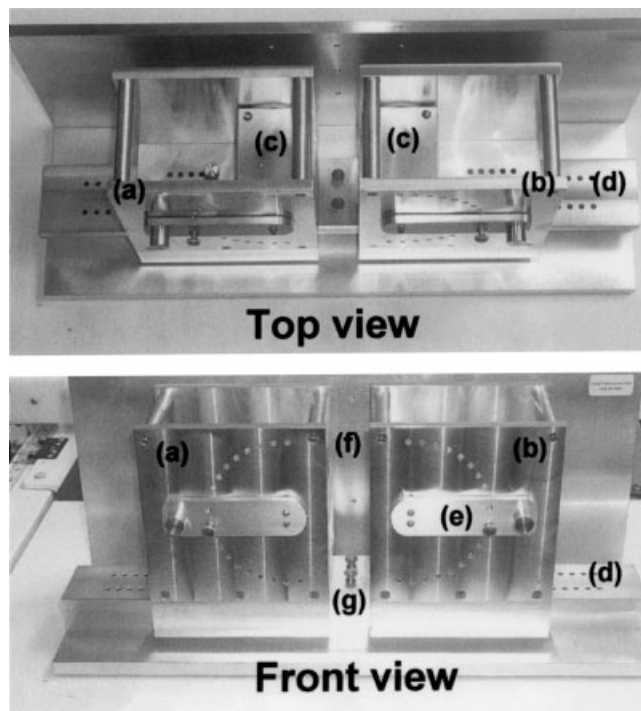

Fig. 2. Gradient field exposure device no. 1. The apparatus was built with aluminum parts and brass hardware to avoid any induced field in ferromagnetic materials. Two frames (**a**, **b**) holding one permanent magnet each (**c**) slide on a rail (**d**). The two magnets can be rotated with a lever (**e**) in steps of 5°. The aluminum back (**f**) accepts various adapters as appropriate for different assays. It currently supports one or a simultaneous set of four culture dishes, or a single Eppendorf tube with a flow-through water jacket for temperature control. An aluminum block (**g**) keeps the two magnets from getting too close to each other.

gradient of the field amplitude lies in that plane because of the symmetrically placed magnets.

Two types of exposure devices (nos. 1 and 2) were designed and built to comply with the requirements outlined above (Robert Jones, Inland Technical Services, San Bernardino, CA).

DEVICE NO. 1

Device no. 1 (Fig. 2) was constructed in aluminum with brass hardware using cylindrical NdFeB magnets that are 25.4 mm tall and have a diameter of 50.8 mm (Tridus, Rancho Domingues, CA). We calculated the dosimetry for device no. 1 in three steps:

1. The field in the planes "B" of Figure 1 was recorded with a three-axis scanner (Redcliffe Magtronics Ltd., Bristol, UK) over an area 300 mm × 300 mm to a resolution of 0.5 mm × 0.5 mm for angles in the range 0–90° in steps of 10°. The field scans were centered on the geometrical center of the magnets.
2. Field and gradient properties were calculated by continuation in planes above the scan plane out to 80 mm in steps of 1.0 mm (Engström, 2001).
3. For each device setting, the resulting fields were projected to the appropriate location in the exposure volume. Distributions and summary statistics (mean and standard deviation for field and gradient

amplitudes) were calculated for the various exposure volumes (areas in cell culture dishes, volume in Eppendorf tube).

The calculated dosimetry was checked with a single axis teslameter (F.W. Bell model 4048) mounted on a micromanipulator. For fields measured in the configuration where the magnets have opposing magnetization, as in Figure 1, a one axis probe is sufficient since the field vector is normal to the symmetry plane "A." Some differences from the calculated values were found; the calculated values were 5–10% lower than the actual measured field. A possible source of error is that the field scan had to be limited to 300 mm × 300 mm, the maximum area of the field scanner available to us; but the field continuation technique depends on knowing the field out to a low cut-off point. The range of possible exposures in the symmetrical mode described here is illustrated in Figure 3.
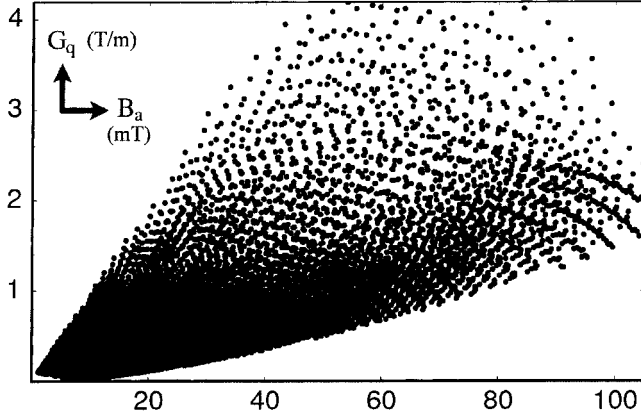
Fig. 3. Range of available exposure conditions for device no. 1. Each point represents a unique exposure condition achieved by varying the parameters (α,d,z) of Figure 1. The values show an average over a 100 μl volume at the bottom of a 1.5 ml Eppendorf tube. The points shown also fulfill the selection criterion that the standard deviation of the individual exposure parameters do not exceed 20% of the respective mean. B_a is measured in mT, G_q in T/m.

DEVICE NO. 2

Device no. 2 (Fig. 4) is constructed using Plexiglas with aluminum and brass hardware. Pairs of cylindrical magnets (Rare-earth magnets, Falls Church, VA) of smaller size than those employed for device no. 1 are used in this version. The largest magnet currently sup-
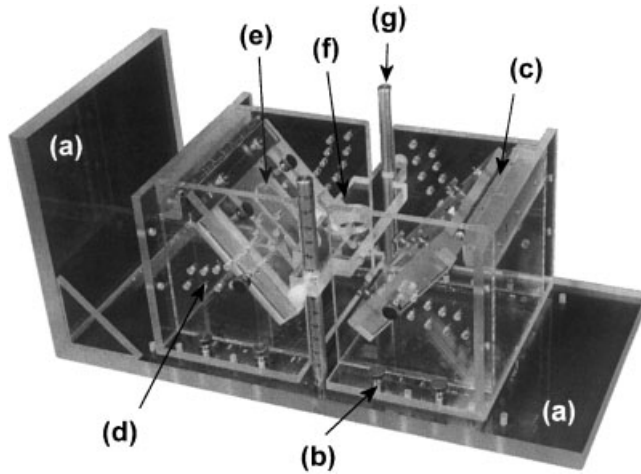

Fig. 4. Gradient field exposure device no. 2. This device was built on an acrylic frame (**a**) with brass and aluminum hardware. There are four adjustable parameters providing three degrees of freedom: separation of the two holders (**b**); angle of the magnet plane (**c**) relative to the exposure location adjustable in 5° steps (**d**). The magnet holder (**e**) allows sliding the magnet relative to the hinge. The exposure location is fixed along the symmetry line (**f**) between the two magnets. Two aluminum rods (**g**) allow vertical positioning of samples.

ported by the device is 6.35 mm tall and has a diameter of 50.8 mm.

Field scans were not obtained for this design. Instead a direct calculation of field properties was performed using a numerical model of appropriately sized NdFeB cylindrical magnets using the finite element modeling software FEMM (Meeker, 2004). Magnetic fields and gradients calculation were simplified by using the cylindrical symmetry of the magnets, for which the field equations are given by Equation 3 below (Engström, 2001):

$$
\begin{aligned}
B_r(r,z) &= \int_0^\infty B_z(r')L_{1r}(r,z,r',z_0)r'\,\mathrm{d}\,r' \\
B_2(r,z) &= \int_0^\infty B_z(r')L_{12}(r,z,r',z_0)r'\,\mathrm{d}\,r'
\end{aligned}
\tag{3}
$$

where the integration kernels are defined by:

$$
\begin{aligned}
L_{1r}(r,z,r') &= \frac{1}{\pi r \alpha_- \alpha_+^2}\left\{ (r^2 - r'^2 - (z - z_0)^2)E(\beta) \right. \\
&\quad \left. + \alpha_+^2 K(\beta)\right\} \\
L_{1z}(r,z,r',z_0) &= \frac{2(z - z_0)}{\pi \alpha_- \alpha_+^2}E(\beta)
\end{aligned}
\tag{4}
$$

The auxiliary variables are

$$
\alpha_-^2 = (r - r')^2 + (z - z_0)^2, \ \alpha_+^2
$$
$$
= (r + r')^2 + (z - z_0)^2, \ \beta = -4rr'/\alpha_-^2.
$$

$K(\beta)$ and $E(\beta)$ are the complete Legendre elliptic integrals of the first and second kinds, respectively (Abramowitz and Stegun, 1972):

$$
K(\beta) = \int_0^{\pi/2} \frac{d\theta}{\sqrt{1 - \beta \sin^2\theta}}
$$

$$
E(\beta) = \int_0^{\pi/2} \sqrt{1 - \beta \sin^2\theta}\,\mathrm{d}\theta
$$

This device is intended to be used in a symmetrical configuration, and the adjustable parameters are (1) the separation of the two magnet holders; (2) the location of the magnet within the holder; (3) the angle of the magnet; (4) the position of the sample perpendicular to the direction the magnet holders are able to move.

Due to the smaller magnets used in this device, the available field levels are lower than what device no. 1 can achieve. Figure 5 shows the field and
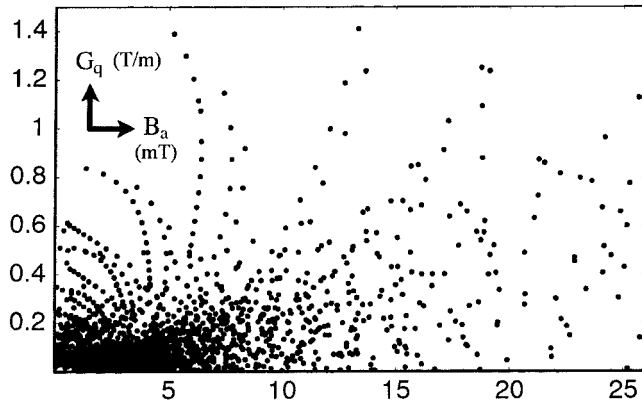
Fig. 5. Range of exposures for device no. 2. Shown are the possible point exposure conditions as the device parameters scan the space of useable combinations. B_a is measured in mT, G_q in T/m.

Fig. 6. Field amplitude (B_a) and perpendicular gradient component (G_q) in device no. 1 when a single parameter is varied. See Figure 1 for a definition of the device parameters. The magnet separation is $2d = 2d' + 100$ mm. **a**: A range of magnet angles, $\alpha \in \{0°, 90°\}$, $d' = 30$ mm, $z = 0$ mm. **b**: Varying the sample position, $\alpha = 40°$, $d' = 20$ mm, $z \in \{-24$ mm, $+24$ mm$\}$. **c**: Changing the magnet separation: $\alpha = 40°$, $d' \in \{10$ mm, 60 mm$\}$, $z = 0$ mm.

gradient ranges for the largest useable magnets (height = 6.35 mm, diameter = 50.8 mm).

Point measurements of the field correspond well with the calculated values.

DISCUSSION

The procedure outlined above provides information about the field given a particular setting (*cf.* Fig. 6), but for the experiment design we had in mind it is necessary to explore change in one field parameter, while other aspects of the field stay constant. To solve this problem, we populated a dosimetry database with all possible device settings for a given exposure geometry, e.g., a 100 µl volume in an Eppendorf tube. This way it is possible to use a database language (SQL) to satisfy a complex set of constraints one may have for experimental design. An example,

> Find two exposure settings such that the first has mean field amplitude larger than 40 mT, with a mean gradient field larger than 1 T/m, and standard deviations of those quantities less than 10% of the respective mean values. Report only those points that also allow finding a second point that approximate the gradient values, but less than half the field amplitude, while keeping the standard deviations of both parameters similar to those of the first point.

The family of pairs of exposures that results from a query such as this are very similar in mean gradients but have distinctly dissimilar mean field amplitude. If we find significant differences between experiments
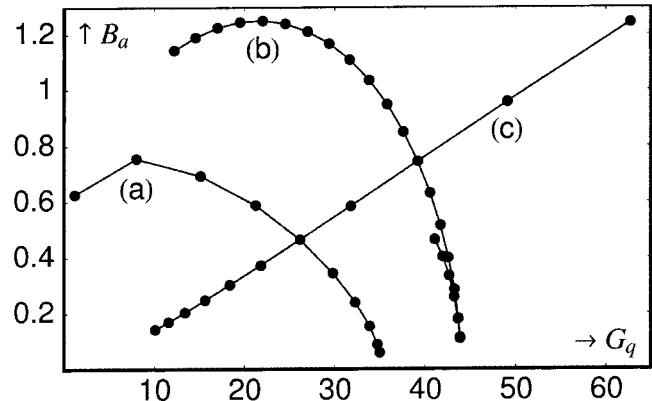
conducted using the two different exposures, we could conclude that field amplitude is indeed a factor for the mechanism responsible for detecting the magnetic field, but not that it is the only factor involved. Similar families of conditions can be found for keeping the field amplitude constant while changing the gradient by a specified amount.

ACKNOWLEDGMENTS

REFERENCES

Abramowitz M, Stegun IA. 1972. Handbook of mathematical functions with formulas, graphs, and mathematical tables. Washington, D.C.: US Government Printing Office.

Cavopol AV, Wamil AW, Holcomb RR, McLean MJ. 1995. Measurement and analysis of static magnetic-fields that block action-potentials in cultured neurons. Bioelectromagnetics 16:197–206.

Engström S. 2001. Green function method for calculating properties of static magnetic fields. Bioelectromagnetics 22:511–518.

Engström S, Markov MS, McLean MJ, Holcomb RR, Markov JM. 2002. Effects of non-uniform static magnetic fields on the rate of myosin phosphorylation. Bioelectromagnetics 23:475–479.

Jackson JD. 1999. Classical electrodynamics. New York, NY: Wiley.

McLean MJ, Holcomb RR, Wamil AW, Pickett JD. 1995. Blockade of sensory neuron action-potentials by a static magnetic-field in the 10 mT range. Bioelectromagnetics 16:20–32.

Meeker DC. 2004. FEMM user manual. URL: http://femm.foster-miller.net.